Adaptive Phase Detrending for GNSS Scintillation Detection: A Case Study Over Antarctica

Luca Spogli, Hossein Ghobadi, Antonio Cicone, Lucilla Alfonsi, Claudio Cesaroni, Nicola Linty, Vincenzo Romano, and Massimo Cafaro, *Senior Member, IEEE*

***Abstract*— We aim at contributing to the reliability of the phase scintillation index on Global Navigation Satellite System (GNSS) signals at high-latitude. To the scope, we leverage on a recently introduced detrending scheme based on the signal decomposition provided by the fast iterative filtering (FIF) technique. This detrending scheme has been demonstrated to enable a fine-tuning of the cutoff frequency for phase detrending used in the phase scintillation index definition. In a single case study based on Galileo data taken by a GNSS ionospheric scintillation monitor receiver (ISMR) in Concordia Station (Antarctica), we investigate how to step ahead of the cutoff frequency optimization. We show how the FIF-based detrending allows deriving adaptive cutoff frequencies, whose value changes minute-by-minute. They are found to range between 0.4 and 1.2 Hz. This allows better accounting for diffractive effects in phase scintillation index calculation and provides a GNSS-based estimation of the relative velocity between satellite and ionospheric irregularities.**

***Index Terms*— Galileo, Global Navigation Satellite Systems (GNSSs), ionosphere, ionospheric irregularities, iterative filtering, modal analysis, signal processing algorithm, transform.**

I. Introduction

THE reliability and accuracy of Global Navigation Satellite System (GNSS) signals in space are threatened by the presence of ionospheric irregularities. They are gradients of electron density embedded in the ambient ionosphere, having typical scale sizes ranging from centimeters up to a few hundreds of kilometers. When a planar wave crosses such irregularities, fluctuations of both amplitude and phase of the received signal at the ground may occur. The Fresnel's filtering mechanism (see [1]–[3]) defines the nature of such fluctuations. Such mechanism makes the Fresnel's scale, being of the order of a few hundred meters for GNSS signals, the fine line between irregularities driving purely refractive fluctuations and those triggering mostly diffractive fluctuations. Specifically, above Fresnel's scale the variation of the refractive index of the ionosphere results in refraction. In this frequency range, the stochastic component of ionospheric effects driven by large-scale and medium-scale structures can be efficiently monitored by using the rate of total electron content (TEC) change index (ROTI), as recently demonstrated by Rino *et al.* [4]. Conversely, below the Fresnel's scale, both diffractive and refractive effects occur. Diffraction is due to the fact that small-scale irregularities behave like wave sources [5], resulting in stochastic fluctuations of the received signal at the ground [1].

Currently, an unambiguous definition of phase scintillation is still missing. In [4], phase scintillation is defined as the "residual after extraction of structure that followed the TEC $1/f_c$ frequency dependence." This definition does not make direct use of the standard deviation of the detrended phase of the received signal, as historically introduced by early works on scintillation and routinely monitored through σ_Φ index by ionospheric scintillation monitor receivers (ISMRs) (see [6], [8]). Because of the need of a phase detrending, the use of σ_Φ implicitly requires a definition of the phase scintillation based on the frequency content, while the definition by Rino *et al.* [4] leverages on the frequency dependence. It is out of the scope of this letter to revise and compare the two definitions, even if some considerations are provided in the conclusions section. Bearing this in mind, we adopt the definition based on the frequency content and we base this work on some recent literature (see [9]–[11]), which tends to call "ionospheric scintillation" only those phase and amplitude fluctuations due to small-scale irregularities. Those are the most challenging threats to GNSS-based positioning services (see [12], [13]). The scintillation is usually quantified through the amplitude and phase scintillation indices, termed S_4 and σ_Φ, respectively [14]. The former is the standard deviation of the normalized signal intensity, while the latter has been defined above.

This work is framed into the recent efforts made by the community to find a proper detrending scheme aimed at serving both science and application. In this context, we aim

Manuscript received September 15, 2020; revised December 14, 2020 and March 1, 2021; accepted March 17, 2021. Date of publication April 2, 2021; date of current version January 5, 2022. This work was supported by the TREASURE, a project funded by the European Union's Horizon 2020 Research and Innovation Program through the Marie Skłodowska-Curie Actions under Grant 722023 (http://ww.treasure-gnss.eu). The work of Antonio Cicone was supported by the Italian Space Agency under Contract ASI "LIMADOU scienza" n 2016-16-H0. *(Corresponding author: Luca Spogli.)*

Luca Spogli and Vincenzo Romano are with the Istituto Nazionale di Geofisica e Vulcanologia, 00143 Rome, Italy, and also with SpacEarth Technology, 00143 Rome, Italy (e-mail: luca.spogli@ingv.it; vincenzo.romano@ingv.it).

Hossein Ghobadi, Lucilla Alfonsi, and Claudio Cesaroni are with the Istituto Nazionale di Geofisica e Vulcanologia, 00143 Rome, Italy (e-mail: hossein.ghobadi@ingv.it; lucilla.alfonsi@ingv.it; claudio.cesaroni@ingv.it).

Antonio Cicone is with the Department of Information Engineering, Computer Science and Mathematics, University of L'Aquila, 67100 L'Aquila, Italy (e-mail: antonio.cicone@univaq.it).

Nicola Linty is with the Finnish Geospatial Research Institute, FI-02430 Masala, Finland (e-mail: nicola.linty@nls.fi).

Massimo Cafaro is with the Department of Engineering for Innovation, University of Salento, 73100 Lecce, Italy, and also with the Istituto Nazionale di Geofisica e Vulcanologia, 00143 Rome, Italy (e-mail: massimo.cafaro@unisalento.it).

Digital Object Identifier 10.1109/LGRS.2021.3067727

at identifying the optimal cutoff frequency ν_c for the retrieval of a σ_Φ which ideally includes only the diffractive portion of the signal phase fluctuations, i.e., the scintillation. This has been demonstrated to be crucial to correctly estimate the ionospheric impact on GNSS data particularly at high-latitude, where the commonly adopted value of 0.1 Hz (see [9]–[11], [15]–[18]) results inappropriate. In the specific, we aim at stepping ahead of what was recently introduced by Ghobadi *et al.* [10]. In this work, a detrending scheme based on the use of the fast iterative filtering (FIF) technique (see [19], [20]) was demonstrated to be effective in providing an adaptive value of the cutoff frequency for each considered radio link. By considering one of the case events analyzed in [10], we demonstrate that the detrending scheme can be further improved by making it adaptive not only per each satellite, but also per epoch, to investigate the temporal variability of the cutoff frequency. This to account for the different nature and features of the ionospheric irregularities that each ray path crosses. In this letter, we prove on a single case event how the FIF-based detrending is able to improve the reliability of the σ_Φ, tuning the disentanglement of the bulk of the refractive effects from phase measurements on a minute-by-minute basis. Such evaluation of $\nu_c = \nu_c(t)$ also enables an estimate of the relative velocity between satellite and ionospheric irregularities.

II. Data and Method

We leverage on the Galileo E01 data (E1 and E5a frequencies) recorded by an ISMR located in Concordia Station (Antarctica, 75.10° S, 123.33° E) and owned by the Istituto Nazionale di Geofisica e Vulcanologia, Rome, Italy [7]. Such ISMR is a Septentrio PolaRxS [8], which records the raw phase and postcorrelation I and Q samples acquired at 50 Hz. Considered E01 data are the same investigated in [10], i.e., those recorded between 14:45 and 15:15 UT of September 8, 2017. In this range, the effects of small- and large-scale irregularities on the signal fluctuations concur and a value of $\nu_C = 0.73$ Hz has been determined in [10]. Such irregularities are likely generated by the intense geomagnetic storm that occurred in early September 2017 [21]. Here, we remind that FIF is able to decompose any nonstationary nonlinear signal s into oscillating modes (intrinsic mode components, IMCs) characterized by their own frequency ν

$$s = \sum_{i=1}^{N_{\mathrm{IMC}}} \mathrm{IMC}_i(\nu) + \mathrm{res} \tag{1}$$

in which N_{IMC} is the total number of found IMCs and res is a residual, that is discarded.

The convergence and stability of FIF was recently proved [23]. We strongly rely on the physical meaning of the modes/frequencies found by FIF to draw the multiscale properties of the ionosphere and exactly identify the Fresnel's frequency ν_F, which is assumed to be the right cutoff frequency to adopt [16]. For our purposes, we use the same results of the FIF decomposition defined by [10, eq. (8)] on the selected data chop.

The FIF-based detrending scheme relies on the power spectral densities (PSDs) of the raw phases (E1 and E5a Galileo signals) and of the corresponding ionosphere free linear combination (IFLC). The IFLC is defined as follows:

$$\mathrm{IFLC} = \frac{\Phi_1 f_1^2 - \Phi_2 f_2^2}{f_1^2 - f_2^2} \tag{2}$$

in which Φ_1 and Φ_2 are the phases of the first (f_1) and second (f_2) central frequencies, respectively. In our case, the first central frequency is E1 (1575.42 MHz) and the second is E5a (1176.45 MHz).

The PSD is obtained by considering the relative energy E_{rel} of all IMCs [10], according to the following formula:

$$E_{\mathrm{rel}}^k(\nu^*) = \frac{< \mathrm{IMC}_k^2(\nu^*) >}{< \sum_{i=1}^{N_{\mathrm{IMC}}} \mathrm{IMC}_i^2(\nu) >} \tag{3}$$

in which k is the index indicating the IMC having frequency ν^*.

The frequency at which the PSD of the IFLC goes below the phase PSD is assumed to be the right cutoff frequency to adopt. This is because, by definition ("iono-free"), IFLC accounts for the dependence of the deterministic ionospheric refractive effects, while stochastic ones do not present such dependence. In addition, the PSD of the signal amplitude is used as a mean of verification, as its peak identifies the Fresnel's frequency [5]. We remind the reader that PSD slightly depends on the type of receivers (bandwidth of the phase lock loop, type of oscillator and corresponding noise, the firmware, etc.). However, the technique can be universally applied because, despite the shape of PDSs may slightly change by changing the receiver, the crossing point among them would (significantly) not. The only caveat of the technique is due to the fact the colored noise may mimic scintillation spectra and affect the proposed technique. Thus, scintillation should be first identified in amplitude, to limit the possibility of misidentified "phase scintillation" due to phase-locked loop colored noise.

In our analysis, we consider the PSDs of raw phase, amplitude, and IFLC as obtained by windowing the IMCs of each time series into subsets of $\Delta t = 1$ min each (corresponding to 3000 raw samples), to retrieve then a value of ν_C that varies with time. Regarding this windowing, here we recall that, differently from standard signal processing methods, FIF allows to first decompose the entire signal and then study them locally, avoiding any issue related to the Gibb's phenomenon at the boundaries. By considering 1-min intervals, we implicitly assume that the ionospheric irregularities spanned by the ray-path in such a time window do not change their stochastic or deterministic nature. What we do not know *a priori* is whether 3000 samples are enough to provide a robust estimation of the PSDs, fulfilling the proposed detrending scheme. Bearing this in mind, σ_ϕ can be calculated by considering, for each interval Δt, the standard deviation of the detrended phase Φ_{detr}, defined as $\Phi_{\mathrm{detr}}(\Delta t) = \sum_i \mathrm{IMC}_i^{\nu \geq \nu_c(\Delta t)}(\Delta t)$, in which the sum is intended on all the IMCs having $\nu \geq \nu_c(\Delta t)$, where $\nu_c(\Delta t)$ indicates the time-varying cutoff frequency.

The mean to verify the improvement with respect to the fixed cutoff is to observe the correlation of σ_ϕ with S_4, that must be better in the case of adaptive cutoff [10]. The higher

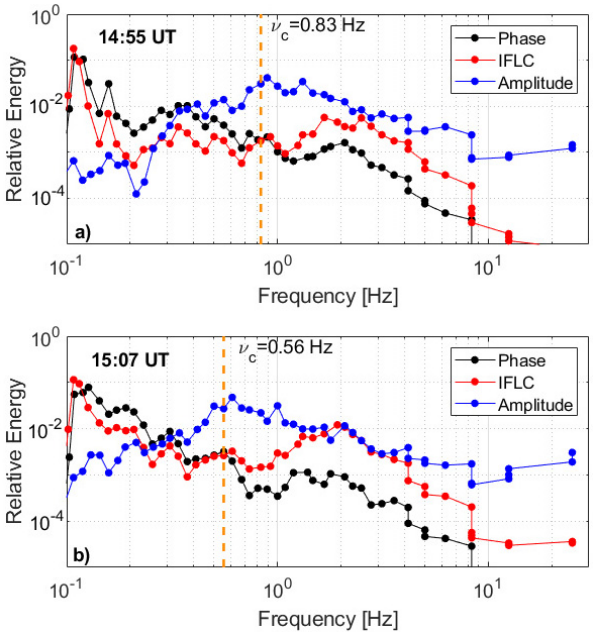

Fig. 1. Two examples of 1-min relative energy for phase (black) and amplitude (blue) at E1 frequency and of IFLC (red) based on E1 and E5a frequencies. (a) Minute ending at 14:55 UT. (b) Minute ending at 15:07 UT, while the orange dashed line indicates the value of ν_C (also given in the text box on the top).

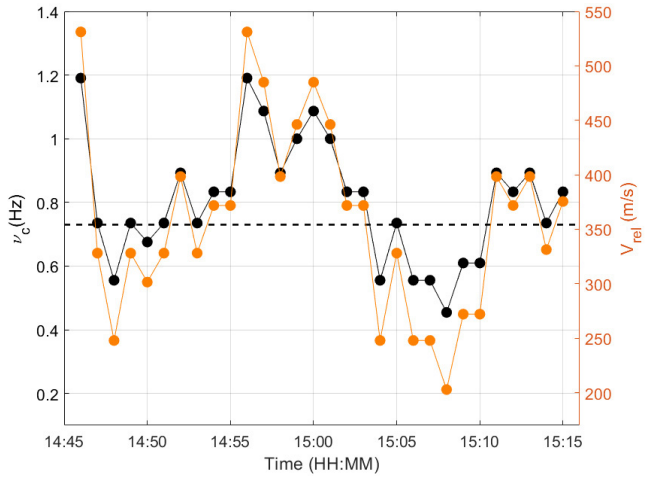

Fig. 2. Time profile of ν_c (black) and of the corresponding value of V_{rel} (orange). The black dashed line indicates the value of 0.73 Hz found in [9].

the correlation, the more efficient is the inclusion of the stochastic effects coming mainly from diffraction effects in the σ_ϕ determination [15].

From the retrieved time series of ν_c, we are also able to provide an estimate of the absolute value of the relative velocity V_{rel} between the irregularity velocity and the ionospheric pierce point (IPP) velocity [16], through the relation $V_{rel} = \nu_F \cdot d_F$, where we assume $\nu_C \equiv \nu_F$ and we consider the far-field geometry and single-thin layer (located at 350 km) approximations. According to this, the Fresnel's distance is $d_F = (2\lambda D)^{1/2}$, where λ is the wavelength and D is the distance between the receiver and the IPP at the ionospheric thin layer (350 km). Bearing this in mind, we remind also that, if not properly evaluated, σ_ϕ has a strong dependence on the plasma convection [22]. The order of magnitude of the speed of such convection is provided by V_{rel}. This strong dependence is actually due to the fact that, if σ_ϕ is calculated with the traditional approach, it depends on the difference between 0.1 Hz and the Fresnel's frequency, which is conversely dependent on the plasma convection velocity.

III. Results

Fig. 1 shows two examples over the 30 retrieved for the case event. Each example presents the relative energy of IMCs for the phase and amplitude of E1 frequency and for the IFLC (E1 and E5a). They refer to the minute ending at 14:55 and 15:07 UT, respectively. In both (as in all the considered PSDs, not shown for brevity reason) examples, the crossing point between the phase and the IFLC spectra is indicated with an orange dashed line. The identified value of ν_c is also reported in a textbox inside each figure. As expected, in both cases the value of ν_c is found in the vicinity of the peak of the amplitude spectrum. This indicates that 3000 samples are enough to build the spectra and identify the cutoff frequency. In the considered examples, the values (0.83 Hz and 0.56 Hz) are different from the fixed value at 0.73 Hz determined in [10] and are again significantly larger than 0.1 Hz, value traditionally adopted to derive σ_ϕ.

Fig. 2 shows the time profile of the cutoff frequency ν_c over 30 min, as retrieved by considering 30 spectra, one for each 1-min interval, separately. The values vary in a quite broad range, i.e., between 0.4 Hz and 1.2 Hz, and are spread around 0.73 Hz (black dashed line in Fig. 2) found in [9].

This is somehow expected, because of the highly dynamical environment featuring the polar cap ionosphere during the selected interval. It is also confirmed by looking at the corresponding time profile of the relative velocity V_{rel} between irregularity and IPP velocities, reported in orange in Fig. 2. The values of V_{rel} range between 200 and 550 m/s, whose order of magnitude fits with what expected for high-latitude convection speeds.

Fig. 3 shows the following.

1) The time profile of σ_ϕ, in red, calculated by considering the time-varying values of $\nu_c(\Delta t)$, reported in Fig. 2.
2) The time profile of σ_ϕ, in black, calculated by using the fixed value $\nu_c = 0.73$ Hz, as in [10].
3) The time profile of the 1-min S_4, in blue, corrected for the impact of the thermal noise as per [6, eq. (13)].

Both fixed and adaptive cutoff frequencies result in the determination of a phase scintillation index in good agreement with S_4.

However, as our aim is the provision of a value of σ_ϕ that includes as much as possible the sole stochastic part of the ionosphere-driven effects, we deeper investigate its correlation with S_4, as the latter accounts only for diffractive (stochastic) effects. With this aim, Fig. 4 shows the correlation between S_4 and σ_ϕ calculated by using both the fixed cutoff frequency $\nu_c = 0.73$ Hz (black) and the adaptive cutoff frequency $\nu_c(\Delta t)$ (red). In Fig. 4, also the linear fits and the

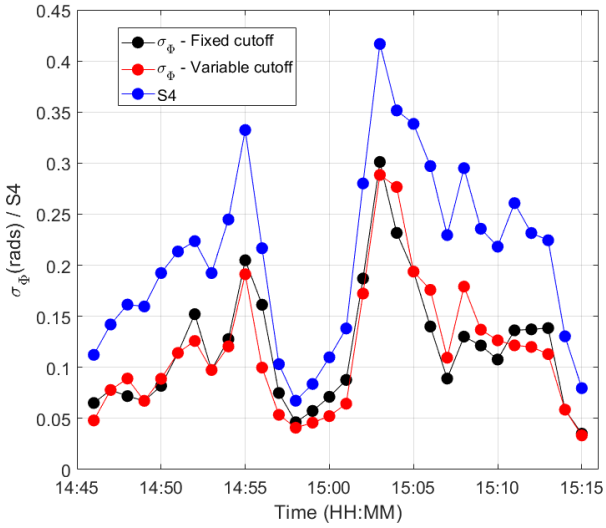

Fig. 3. Time profile of S4 (blue), of σ_Φ calculated by using a fixed value of $\nu_C = 0.73$ Hz (black) and by using a variable cutoff frequency (red).

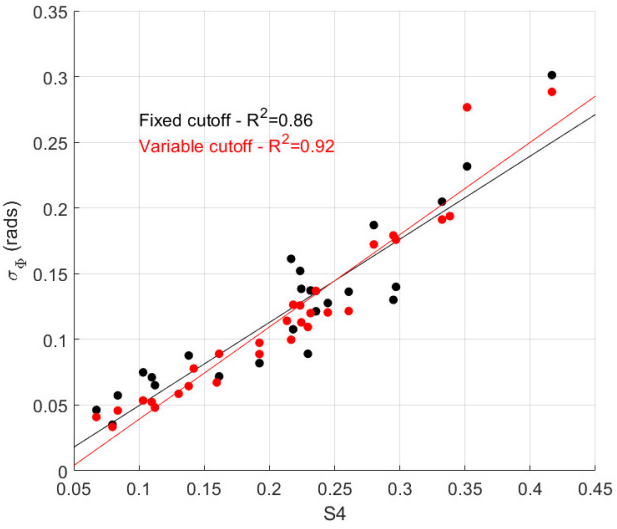

Fig. 4. Correlation between S4 and σ_Φ as calculated by using a fixed value of $\nu_C = 0.73$ Hz (black dots) and by using a variable cutoff frequency (red dots). The solid lines indicate the linear fit whose R^2 is also reported.

corresponding coefficients of determination R^2 are provided. As described in [10, Table 4], the use of the fixed cutoff frequency at 0.73 Hz improves the correlation with respect to the standard cutoff frequency at 0.1 Hz, by raising the R^2 from 0.71 to 0.86. The use of the adaptive cutoff frequency enables further improvement of the correlation, raising this time the coefficient of determination up to 0.92. This confirms that the use of the adaptive cutoff frequency allows retrieving a more reliable value of the phase scintillation index, in terms of its capability in providing information about the stochastic portion of the ionospheric effect, mainly of diffractive origin. According to Fig. 4, the spread around the linear fit is reduced especially in the S_4 range between 0.1 and 0.35. Such spread, should provide a measure of the stochastic effects induced by refraction and triggered by processes occurring above the Fresnel's scale.

IV. Conclusion

We prove, on the basis of a single case study, how the use of an adaptive evaluation of the cutoff frequency for phase detrending is able to improve the determination of the phase scintillation index. This in view of providing an index that accounts only for the most disruptive effects on the phase of GNSS signals, i.e., those due to the stochastic effects triggered by small-scale irregularities. The detrending scheme is based on the use of the FIF signal decomposition technique and improves a similar scheme, presented in [10]. That scheme has improved the cutoff frequency determination by providing a fixed cutoff frequency for each satellite. The use of a fixed cutoff frequency for a ray-path that spans a large portion of the ionosphere is, however, not suitable to account for the different ionospheric conditions crossed by the GNSS signal, especially under stormy conditions. With this aim, we propose to compute a time-varying adaptive cutoff frequency. We investigate the scintillation event on Galileo E01 signal recorded in the polar cap ionosphere over Concordia Station (Antarctica) during the September 2017 storm. We demonstrate that the use of 1 min of raw data taken at 50-Hz sampling rate is sufficient to feed the FIF algorithm and then to derive reliable spectra for the cutoff frequency determination. Such data chop is also enough to cover a single ionospheric sector and to account for the very large spatial and temporal variability of the polar cap ionosphere.

Further studies are needed for the statistical assessment of our results which can enable real-time implementation of the proposed detrending scheme in the next generation of scintillation receivers and dedicated infrastructures [24]. In addition, the technique can be also used on shorter time windows (e.g., 10 s) to account for shorter variations that are driven by sudden events or occurring in the high-latitude ionosphere (see [25], [26]).

As a concluding remark, we remind here that this study is based on two hypothesis: 1) the definition of phase scintillation based on the frequency content and not on the frequency dependence [4] and 2) the assumption that IFLC is able to account for all refractive fluctuations triggered by the ionosphere. If (2) is satisfied, the two definitions of scintillation coincide. As discussed in [4], this is the case for weak to moderate scintillation conditions that result in single phase screen approximation. When wave scattering through multiple phase screens is present, the two definitions diverge because stochastic fluctuations from medium and large scale irregularities are found [4] and IFLC is not completely effective in accounting for variations driven by the irregularities of such a scale. While Rino *et al.* [4] present a preliminary assessment of the impact on positioning in terms of TEC error, a thorough assessment of the phase scintillation impact, defined in the different reported ways, is still missing in the literature and worth to be further investigated. In this work, we aimed at showing also the limitations on the use of σ_ϕ, which include, beside the selection of a proper cutoff frequency for phase detrending, also a strong link with the receiver features. This to advise about an index that is still widely used in the community, both to characterize the features of ionospheric irregularities and to adopt mitigation solutions.

ACKNOWLEDGMENT

The authors thank Programma Nazionale di Ricerche in Antartide (PNRA) for supporting the upper atmosphere observations at Concordia Station (Antarctica). This work has been conducted in the frame of the TREASURE Project (http://www.treasure-gnss.eu/), a prestigious Marie Skłodowska-Curie Actions (MSCA) Innovative Training Network (ITN). The fast iterative filtering (FIF) algorithm, available for the public at: https://github.com/Acicone/FIF, was developed by Dr. Antonio Cicone, who is a member of the Italian "Gruppo Nazionale di Calcolo Scientifico" (GNCS) of the INdAM. A special thanks to Dr. Giorgiana De Franceschi for her kind support, which inspired this work, and to Charles Rino, for the precious comments on the work that significantly improved it.

REFERENCES

[1] C. L. Rino, "A power law phase screen model for ionospheric scintillation: 1. Weak scatter," *Radio Sci.*, vol. 14, no. 6, pp. 1135–1145, Nov. 1979.

[2] V. E. Gherm and N. N. Zernov, "Fresnel filtering in HF ionospheric reflection channel," *Radio Sci.*, vol. 30, no. 1, pp. 127–134, Jan. 1995.

[3] E. J. Fremouw, "Geometrical control of the ratio of intensity and phase scintillation indices," *J. Atmos. Terr. Phys.*, vol. 42, nos. 9–10, pp. 775–782, Sep. 1980.

[4] C. Rino, Y. Morton, B. Breitsch, and C. Carrano, "Stochastic TEC structure characterization," *J. Geophys. Res., Space Phys.*, vol. 124, no. 12, pp. 10571–10579, Dec. 2019.

[5] A. W. Wernik, J. A. Secan, and E. J. Fremouw, "Ionospheric irregularities and scintillation," *Adv. Space Res.*, vol. 31, no. 4, pp. 971–981, Jan. 2003.

[6] A. J. Q. Van Dierendonck, J. Klobuchar, and Q. Hua, "Ionospheric scintillation monitoring using commercial single frequency C/A code receivers," in *Proc. ION GPS*, vol. 93, 1993, pp. 1333–1342.

[7] Upper Atmosphere Physics and Radiopropagation Working Group, "Electronic space weather upper atmosphere database (eSWua)—GNSS scintillation data, version 1.0," Istituto Nazionale di Geofisica e Vulcanologia, Rome, Italy, Aug. 2020, doi: 10.13127/ESWUA/GNSS.

[8] B. Bougard, J. M. Sleewaegen, L. Spogli, S. V. Veettil, and J. F. Monico, "CIGALA: Challenging the solar maximum in Brazil with PolaRxS," in *Proc. 24th Int. Tech. Meeting Satell. Division Inst. Navigat.*, 2011, pp. 2572–2579.

[9] G. D. Franceschi, L. Spogli, L. Alfonsi, V. Romano, C. Cesaroni, and I. Hunstad, "The ionospheric irregularities climatology over Svalbard from solar cycle 23," *Sci. Rep.*, vol. 9, no. 1, pp. 1–14, 2019.

[10] H. Ghobadi *et al.*, "Disentangling ionospheric refraction and diffraction effects in GNSS raw phase through fast iterative filtering technique," *GPS Solutions*, vol. 24, no. 3, pp. 1–16, Jul. 2020.

[11] A. M. McCaffrey and P. T. Jayachandran, "Determination of the refractive contribution to GPS phase 'scintillation,'" *J. Geophys. Res., Space Phys.*, vol. 124, no. 2, pp. 1454–1469, Feb. 2019.

[12] V. E. Gherm, N. N. Zernov, and H. J. Strangeways, "Effects of diffraction by ionospheric electron density irregularities on the range error in GNSS dual-frequency positioning and phase decorrelation," *Radio Sci.*, vol. 46, no. 3, pp. 1–10, Jun. 2011.

[13] M. V. Tinin, "Eliminating diffraction effects during multi-frequency correction in global navigation satellite systems," *J. Geodesy*, vol. 89, no. 5, pp. 491–503, May 2015.

[14] E. J. Fremouw *et al.*, "Early results from the DNA wideband satellite experiment-complex-signal scintillation," *Radio Sci.*, vol. 13, no. 1, pp. 167–187, Jan. 1978.

[15] T. L. Beach, "Perils of the GPS phase scintillation index ($\sigma\phi$)," *Radio Sci.*, vol. 41, no. 5, pp. 1–7, 2006.

[16] B. Forte and S. M. Radicella, "Problems in data treatment for ionospheric scintillation measurements," *Radio Sci.*, vol. 37, no. 6, pp. 1–8, 2002.

[17] B. Forte, "Optimum detrending of raw GPS data for scintillation measurements at auroral latitudes," *J. Atmos. Sol.-Terr. Phys.*, vol. 67, no. 12, pp. 1100–1109, Aug. 2005.

[18] S. C. Mushini, P. T. Jayachandran, R. B. Langley, J. W. MacDougall, and D. Pokhotelov, "Improved amplitude- and phase-scintillation indices derived from wavelet detrended high-latitude GPS data," *GPS Solutions*, vol. 16, no. 3, pp. 363–373, Jul. 2012.

[19] L. Lin, Y. Wang, and H. Zhou, "Iterative filtering as an alternative algorithm for empirical mode decomposition," *Adv. Adapt. Data Anal.*, vol. 1, no. 4, pp. 543–560, 2009.

[20] A. Cicone, "Iterative filtering as a direct method for the decomposition of nonstationary signals," *Numer. Algorithms*, vol. 85, no. 3, pp. 811–827, 2020.

[21] N. Linty, A. Minetto, F. Dovis, and L. Spogli, "Effects of phase scintillation on the GNSS positioning error during the September 2017 storm at Svalbard," *Space Weather*, vol. 16, no. 9, pp. 1317–1329, Sep. 2018.

[22] Y. Wang *et al.*, "Experimental evidence on the dependence of the standard GPS phase scintillation index on the ionospheric plasma drift around noon sector of the polar ionosphere," *J. Geophys. Res., Space Phys.*, vol. 123, no. 3, pp. 2370–2378, Mar. 2018.

[23] A. Cicone and P. Dell'Acqua, "Study of boundary conditions in the iterative filtering method for the decomposition of nonstationary signals," *J. Comput. Appl. Math.*, vol. 373, Aug. 2020, Art. no. 112248.

[24] H. Ghobadi *et al.*, "User-oriented ICT cloud architecture for high-accuracy GNSS-based services," *Sensors*, vol. 19, no. 11, p. 2635, Jun. 2019.

[25] M. Materassi and C. N. Mitchell, "Wavelet analysis of GPS amplitude scintillation: A case study," *Radio Sci.*, vol. 42, no. 1, pp. 1–10, 2007.

[26] A. M. Smith *et al.*, "GPS scintillation in the high arctic associated with an auroral arc," *Space Weather*, vol. 6, no. 3, pp. 1–7, Mar. 2008.